

Photonic crystal-based smart contact lens for continuous intraocular pressure monitoring

Bohee Maeng^a, Hyung-Kwan Chang^a and Jungyul Park^{*a}

Department of Mechanical Engineering, Sogang University, 35 Baekbeom-or, Mapo-gu, Seoul 04107, Republic of Korea.

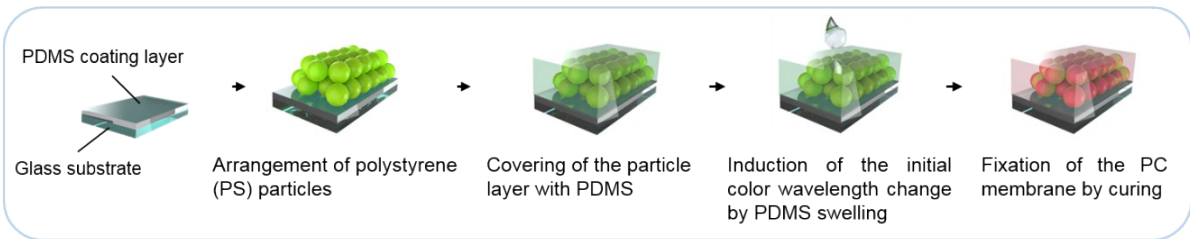
* Corresponding author: Prof. Jungyul Park

E-mail: sortpark@sogang.ac.kr

Phone: +82-2-705-8642

Full postal address: Room 705, Adam Shall Hall, Department of Mechanical Engineering, Sogang University, 35 Baekbeom-or, Mapo-gu, Seoul 04107, Republic of Korea.

A Fabrication process of the photonic crystal-embedded ultrathin PDMS membrane



B Fabrication process of the smart contact lens

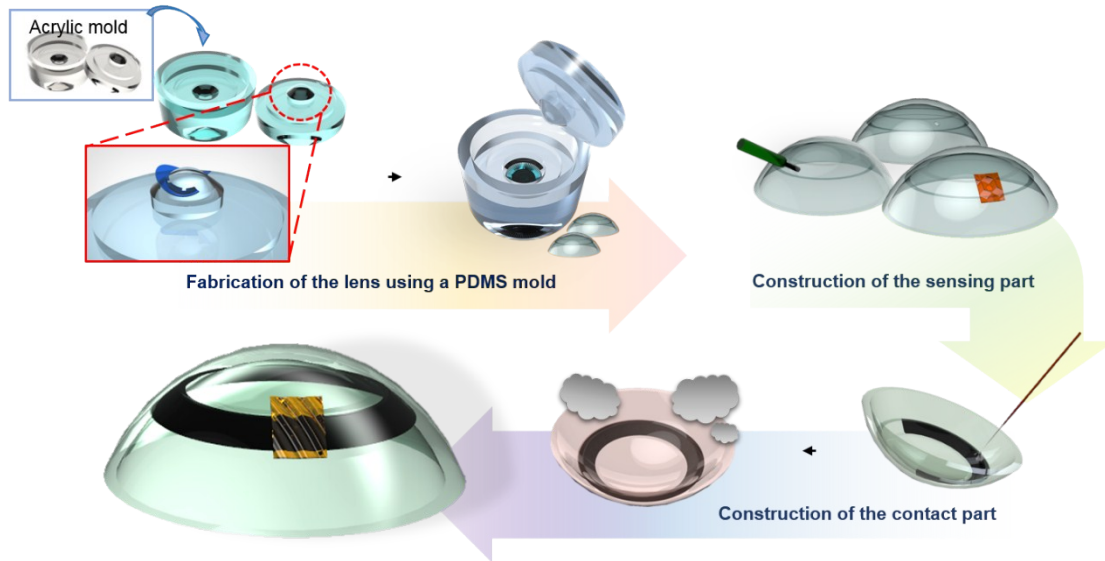


Fig. S1 Fabrication of the smart contact lens sensor, which consists of the microfluidic amplification system. A) Fabrication process of the photonic crystal-embedded thin PDMS membrane for the sensing part of the lens. B) Fabrication process for the smart contact lens: to make the lens, Ostemer solution was injected into a PDMS mold made from an acrylic structure. A hole was drilled in the ring-shaped channel of the lens removed from the mold and covered with a PC membrane to create a sensing part for observing the color change. When the channel was filled with silicone oil and a parylene deposition was applied to it, the lens with a microhydraulic amplification system was completed.

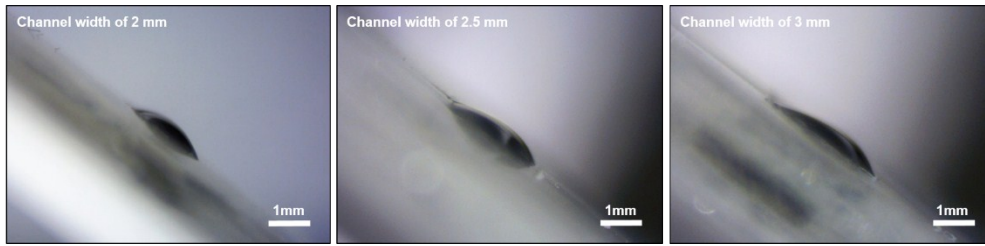


Fig. S2 Cross-sectional images of silicone oil loaded in inclined artificial channels. The slope of the channels (38°) was the same as the ring-shaped channel of the smart contact lens. The channel widths were 2, 2.5 and 3 mm. The silicone oil was loaded convexly, just as it would fill the smart contact lens channel. The loaded oil in 2 mm channel shows symmetric dome shape but the other cases tilted dome shape.

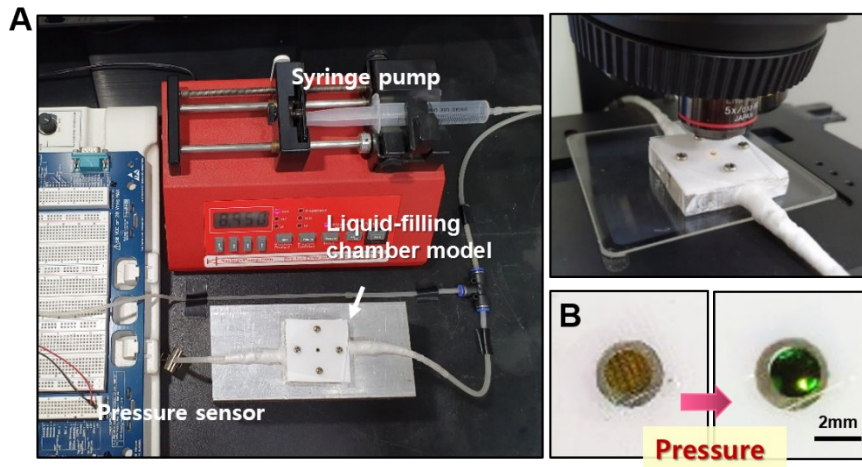


Fig. S3 Determination of the optimal hole size of the sensing part. A) Images of experimental set up for investigating the wavelength change of the PC membrane. B) Images of PC membrane before (left) and after (right) applying pressure.

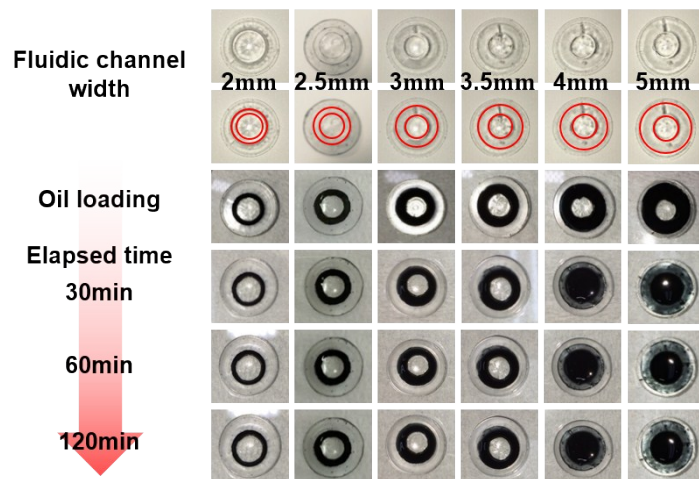


Fig. S4 Exploration of the optimal area of the contact part. Pictures demonstrating the widths of the ring-shaped channel that allows the silicone oil to stay in the channel without overflowing. They show conditions of the silicone oil filled in the ring-shaped 2- to 5-mm wide channels over time.

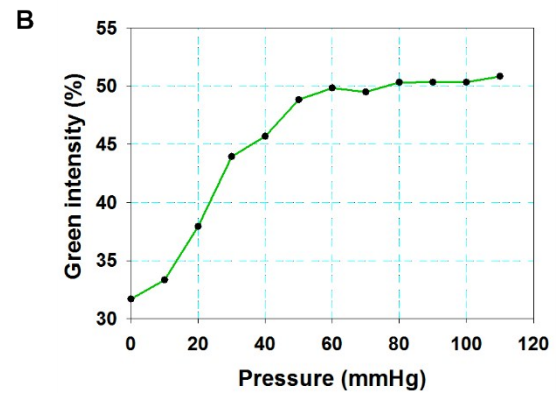
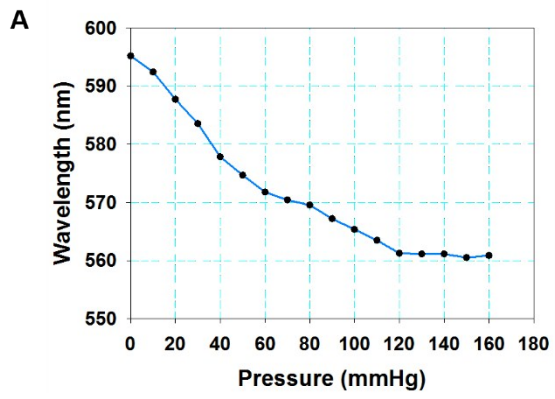


Fig. S5 Evaluation of the detection range of smart contact lens with a A) spectrometer and B) smartphone camera in the *in vitro* tests.

< Numerical simulation >

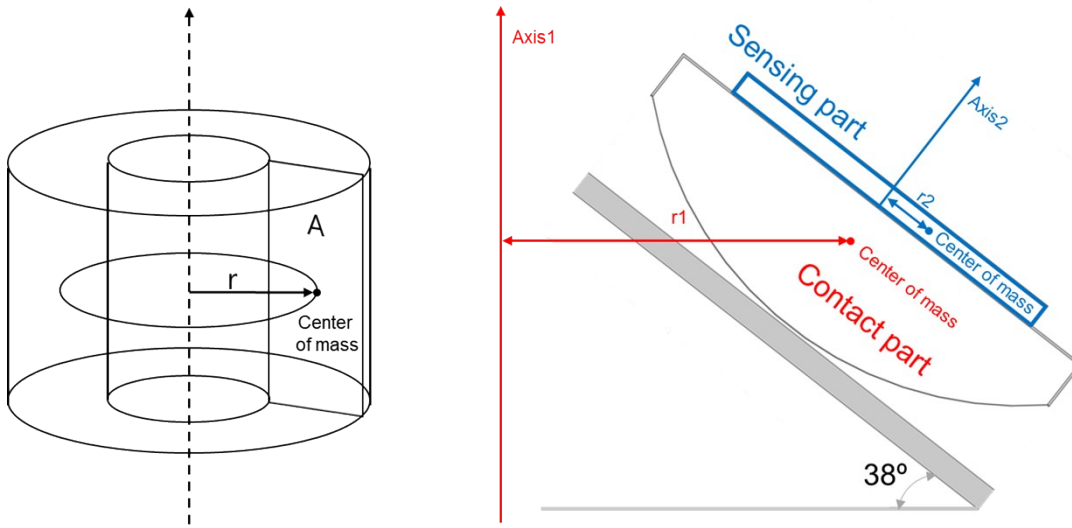


Fig. S6 Calculation of volume from 2d axial symmetry structure using center of mass and model of proposed device.

Table S1 Simulation result

Displacement of cornea [μm]	Volume of contact part [mm ³]	Area of contact part [mm ²]	Strain [Δt/t ₀]	Center of mass Contact part (r1) [mm]	Center of mass Sensing part (r2) [mm]	Displacement of sensing part [μm]
Channel width 2 mm						
0	34.141	0.930	0.0000	5.8404	0.3749	0
30	34.103	0.929	-0.0028	5.8419	0.3490	49
60	34.053	0.927	-0.0130	5.8440	0.3340	105
Channel width 2.5 mm						
0	40.595	1.100	0.0000	5.8714	0.3750	0
30	40.567	1.103	-0.0016	5.8518	0.3536	37
60	40.519	1.102	-0.0098	5.8525	0.3369	92
Channel width 3.0 mm						
0	52.688	1.427	0.0000	5.8755	0.3750	0
30	52.675	1.435	-0.0004	5.8431	0.3620	20
60	52.630	1.434	-0.0060	5.8401	0.3419	72